International Journal of Nanoelectronics and Materials
IJNeaM
ISSN 1985-5761 | E-ISSN 2232-1535

Investigation of blend ratios on physical, mechanical, and electrical properties of stretchable conductive ternary blend NRL/VSR materials: Unfilled and filled system

Wern-Ming Che [a], Pei Leng Teh [a,b *], Jalilah Binti Abd Jalil [a], Cheow Keat Yeoh [a,b], and Mohamad Nur Fuadi Bin Pargi [C]

[a] *Faculty of Chemical Engineering & Technology, Universiti Malaysia Perlis, Arau, 02600, Perlis, Malaysia.*
[b] *Centre of Excellence for Frontier Materials Research (CFMR), Universiti Malaysia Perlis, Arau, 02600, Perlis, Malaysia.*
c Faculty of Innovative Design and Technology, Universiti Sultan Zainal Abidin, Kampus Gong Badak, 21300 Kuala Nerus, Terengganu Darul Iman
∗Corresponding author. Tel.: +60-12-678-0329; e-mail: plteh@unimap.edu.my

Received 18 January 2024, Revised 23 April 2024, Accepted 13 May 2024

ABSTRACT

Stretchable conductive material has garnered significant attention in recent years since it offers both electrical conductivity and the ability to undergo significant deformation without losing its conductivity. Herein, NRL/VSR blend materials were prepared with varying blend ratios, both with and without GNP-SDS, using a simple mechanical stirring method. The main objective was to investigate the influence of blend ratios on the physical, mechanical, and electrical properties of the unfilled and filled blend systems. The findings revealed that the addition of VSR had a detrimental effect on the crosslink density of the resulting materials, leading to a negative impact on their mechanical properties. However, a contrasting observation was made regarding the electrical properties. The introduction of VSR induced the formation of a double percolation structure in the immiscible NRL/VSR blend. This double percolation structure facilitated the creation of a conductive network within the blend, which significantly improved its electrical properties by approximately 263.85 folds.

Keywords: *Natural rubber latex; Vulcanized silicone rubber; Graphene nanoplatelet; Double percolation*

1. INTRODUCTION

Stretchable conductive materials have garnered significant interest due to their ability to endure substantial deformations while retaining product functionality. The prevailing technique for fabricating these materials involves incorporating conductive particles into elastomeric materials using the common methods for example: mechanical mixing [1], 3D printing [2] and solution casting methods [3]. Natural rubber latex (NRL), a white sap obtained from the *Hevea brasiliensis* tree, offers high elasticity and mechanical strength once its cis-1,4-polyisoprene chains undergo crosslinking with suitable curing additives [4]. However, NRL has low thermal and ozone resistance and is typically used as an insulator.

To address this limitation, graphene nanoplatelets (GNPs) were selected as the conductive particles to be added into NRL. GNP has attracted material engineers due to its unique structure and exceptional properties, including a large surface area measuring 2630 m^2/g, high mechanical property with a Young's modulus of 1 TPa, exceptional thermal conductivity reaching 5000 W m/K, and high charge carrier mobility, offering excellent electrical properties [5]. In order to transform NRL into a conductor, a sufficient amount of GNP is required to be added to the matrix to form a continuous conductive network once the filler loading reaches the critical concentration, known as the percolation threshold [6]. However, a high filler loading tends to deteriorate the mechanical properties of the composites.

To overcome this, a double percolation structure can be induced by adding a secondary matrix to create an immiscible ternary blend system [7]. This helps in aligning the conductive particles at the interface to fabricate a highly conductive material with a lower percolation threshold [8]. For this study, silicone rubber (SR) was chosen as the secondary matrix due to its alternating -Si-O- backbone, which imparts high bond strength and provides good thermal, weather, and chemical resistance [9]. Consequently, ternary composites with different NRL/SR blend ratios, filled with 0 phr and 7 phr of GNP, were prepared to investigate the effect of blend ratios on the properties of the unfilled and filled NRL/SR/GNP composites.

2. MATERIALS AND METHODOLOGY

Natural rubber latex (NRL) with a TSC (Total Solid Content) of 60 % was supplied by MG Color Sdn. Bhd. The additives, including zinc oxide (ZnO), zinc diethyldithiocarbamate (ZDEC), zinc 2-mercaptobenzothiazole (ZMBT), and sulphur (S), were purchased from Furben Technique (M) Sdn. Bhd. Stearic acid (SA) was supplied by Acidchem International Sdn. Bhd., and the stabilizer potassium hydroxide (KOH) was purchased from Johchem Scientific & Instruments Sdn. Bhd. Vulcanized silicone rubber powder (VSR) was supplied by Eurochemo-Pharma Sdn. Bhd., while graphene nanoplatelet (0540DX) was purchased from SkySpring Nanomaterials Inc., United States, and sodium sulfate dodecyl (SDS) was purchased from Sigma-Aldrich Corporation.

In the initial step, the GNP was dispersed in a 2 % SDS solution using sonication for 30 minutes, followed by 24 hours of stirring with a magnetic stirrer. After 24 hours, the GNP-SDS mixture was filtered and washed repeatedly with distilled water. Subsequently, the GNP-SDS and additives were added to NRL and stirred overnight. The compounded latex was then filtered, and VSR was added, followed by another 10 minutes of stirring. The resulting mixture was cast onto a glass mold. After 72 hours of curing at room temperature, the casted sheet underwent post-curing in an oven at 70 °C for 24 hours. These steps were replicated with varying blend ratios (100/0, 95/5, 90/10, 85/15, and 80/20) with filler loadings of 0 phr and 7 phr.

3. TESTING AND CHARACTERIZATION

The swelling percentage of the composites was determined by immersing the weighed samples (~0.2 g) in toluene until the equilibrium mass obtained. Then, crosslink density of the composites was calculated by using the Flory-Rehner equation:

$$v = \frac{1}{M_{cs}} = -\left[\frac{V_2 + \chi V_2 + ln(1-V_2)}{\rho_2 V_2 \left(V_2^{\frac{1}{3}} - \frac{1}{2}V_2\right)}\right] \quad (1)$$

Where v is the effective number of moles of crosslinked chains per gram of polymer in mol/g; M_{cs} is the molecular weight between crosslinks in g/mol; V_2 is the volume fraction of polymer in the swollen mass; V_1 is the molar volume of the solvent in ml/mol; χ is the polymer-solvent interaction parameter, while $\boldsymbol{\rho}_2$ is the density of the polymer in g/cm^3.

Moreover, tensile properties were identified by using the Instron 5569 Universal Testing Machines (UTM) according to the ASTM D412. The fracture surface was then observed by using SEM (Jeol JSM 6010LA). Furthermore, the electrical conductivity test was obtained according to the ASTM D257 by using the Fluke 8845A/8846A 6.5-digit precision multimeter in direct current mode with a voltage supply of 5V at room temperature. Then, both the bulk resistivity (R) and bulk conductivity (σ) were calculated by using Equation (2) and Equation (3).

$$R = \frac{r.A}{d} \quad (2)$$

$$\sigma = \frac{1}{.R} \quad (3)$$

Where r is resistance of resistor, A is the area of the specimens in cm^2 and d is the thickness of the specimens in cm.

4. RESULTS AND DISCUSSION

The results presented in Figures 1 and 2 summarize the variation of swelling percentages and crosslink densities for both unfilled and filled NRL/VSR blends. It is observed that the swelling percentage is inversely proportional to the crosslink density. The addition of VSR as the secondary matrix in the blended materials resulted in increased solvent uptake, indicating a reduction in the crosslink density. This can be attributed to the presence of discrete VSR particles, which hindered the approaching of NRL chains during the formation of sulfidic linkages. The loosely crosslinked structure allowed the solvent to penetrate readily [10]. However, the swelling percentage showed a slower decrease with the increment of VSR content due to the better solvent resistance of VSR. This resistance is attributed to the similar solubility parameter (δ) between the NRL [8.12 (cal/cm^3)$^{-2}$] and toluene [8.91 (cal/cm^3)$^{-2}$] [11] which showed a much more similar solubility parameter as compared to the VSR [δ=7.30 (cal/cm^3)$^{-2}$] [12]. Thus, the solvent intake dropped slowly with the increment of VSR proportion. In the case of the filled system, the filler located in the interstitial region of the NRL covered the reactive sites of the NRL chains, interfering with crosslink formation. Additionally, the presence of an interfacial gap between the matrix and the agglomerated GNP-SDS allowed more solvent to penetrate the materials, leading to an overall decline in the crosslink concentration of the NRL matrix [10]. Consequently, this had a negative impact on the properties of the blended materials.

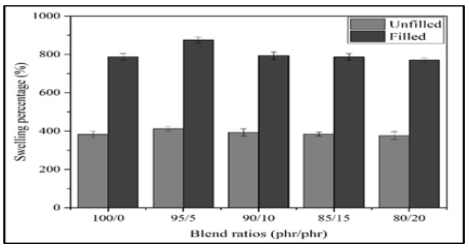

Figure 1 Swelling percentage of unfilled and filled NRL/VSR with varying blend ratios.

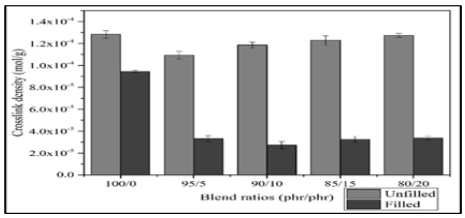

Figure 2 Crosslink density of unfilled and filled NRL/VSR with varying blend ratios.

Figure 3 displays the tensile strength of the unfilled and filled NRL/VSR blend materials at different blend ratios. For the unfilled 95/5 system, the improvement of tensile strength attributed to the larger surface area of the VSR provided additional entanglement to resist the applied force and prevent the failure of the samples [13]. Besides, as the VSR content increased from 10 phr to 20 phr, and the addition of the GNP-SDS spontaneous, the high interfacial tension of the blend components caused the weak interfacial interaction of the components. In addition, the GNP-SDS tended to agglomerate, especially with the presence of VSR, which aligned the GNP-SDS at the NRL-VSR interface, caused the stress concentration at the interface, and led to the failure of the samples to occur readily.[14]. Moreover, the VSR powder tended to form agglomerates rather than disperse within the NRL matrix, assignable to the high cohesive force as shown in the micrograph obtained by the SEM. From the micrograph in Figure 6, the VSR aggregated in certain areas and formed the VSR-rich and VSR-poor regions as the VSR proportion increased to 20 phr. The bounded VSR cluster was insufficient to form strong interfacial interaction with NRL and also increased the heterogeneity of the blend system, which in turn led to the inferior tensile properties of the specimens [15].

The elongation at break, modulus at 300 % elongation (M300), and modulus at 500 % elongation (M500) of the unfilled and filled NRL/VSR materials at different elongations were demonstrated in Figures 4 and 5 respectively. The elongation at break dropped continuously due to the compact structure as both the VSR and GNP-SDS dispersed within the NRL matrix, which then restricted the dislocation of the chains under stress. Hence, the elongation at break dropped with the increment of VSR and GNP-SDS content due to the reduction of chain mobility [16].

On the other hand, the modulus only showed improvement at 5 phr of VSR for both filled and unfilled systems. This could be ascribed to the uniform dispersion of the 5 phr of VSR within the NRL matrix. Physical interaction formed in between the VSR and NRL, resisting the force applied and remaining the chains in their original position. Contrastingly, as the VSR content increased, the highly crosslinked VSR formed larger bundle clusters and aggregated at certain regions [17]. The immiscibility between the matrices provoked the stress concentrator at the interface and accelerated the deformation of the blend materials [18].

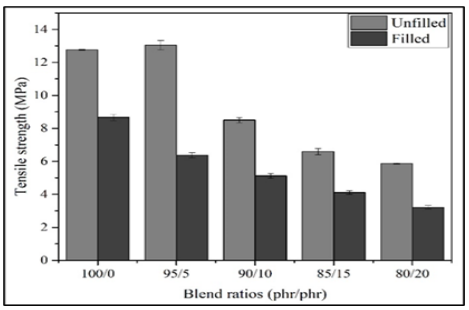

Figure 3 Tensile strength of unfilled and filled NRL/VSR with varying blend ratios.

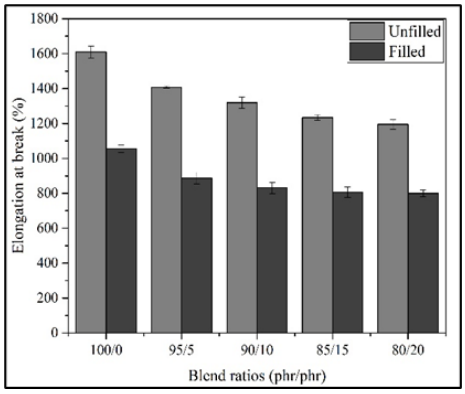

Figure 4 Elongation at the break of unfilled and filled NRL/VSR with varying blend ratios.

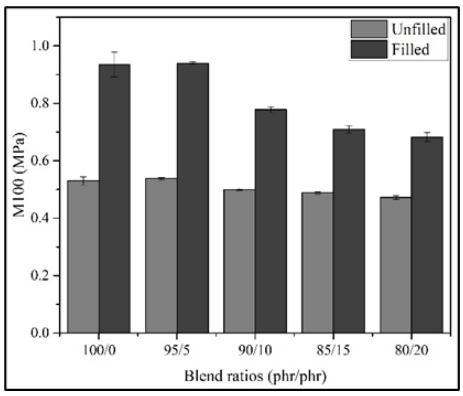

(a)

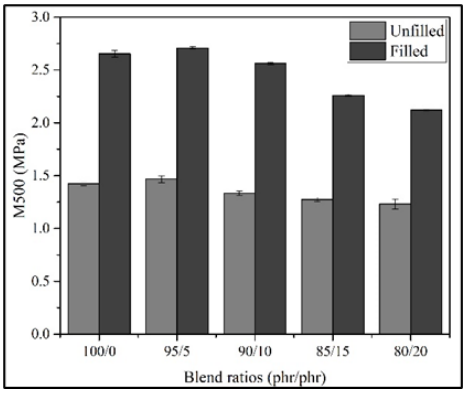

(b)

Figure 5 (a) M100 and (b) M500 of unfilled and filled NRL/VSR with varying blend ratios, respectively.

Figure 6 shows the tensile fractured surface of unfilled and filled NRL/VSR/GNP with different blend ratios magnified at ×1000 magnification. It was found that VSR existed in various sizes, by which the smaller particles were still attached to the NRL surface. Then, some of the larger VSR aggregates had been pulled out under pulling force and left holes on the fracture surface, signifying the weak interfacial interaction between NRL and large VSR aggregates, inducing the formation of an interfacial gap. As aforementioned, this could act as the stress concentration point that accelerated the failure of the specimens.

On the other hand, filler agglomeration was discovered for the filled system. The agglomerated GNP-SDS offered a smaller surface area to interact with the matrix phase.

Hence, a large interfacial gap existed and was captured for the filled system, especially with the existence of VSR. A similar matrix-filler interfacial gap was also found from the outcome of Aiza Jaafar and co-workers [19]. This defined weak interfacial strength between the NRL and GNP-SDS [20]. Hence, inferior tensile properties were shown for the composites with high filler loading.

Figure 7 shows the electrical properties of the unfilled NRL/VSR materials with different NRL/VSR blend ratios. From the result, the addition of VSR into the blend materials diminished the electrical properties of the blend systems. The reduction of the electrical properties is assigned to the higher electrical resistivity of the silicone rubber. According to the research of Kamarudin and coworkers, the surface resistivity of the neat silicone rubber was around 1.37×10^{14} Ω. cm which was far larger than the electrical resistivity of neat NRL [21]. So, as more VSR is added and dispersed within the NRL matrix, the higher the bulk resistivity of the materials and the lower the bulk conductivity.

Then, filled NRL/VSR was prepared by loading the materials with 7 phr of GNP-SDS by varying the blend ratio from 100/0 to 80/20. The electrical properties of the filled NRL/VSR are illustrated in Figure 7 (b). It can be noticed that the addition of VSR gave a positive effect on the electrical properties of the filled NRL/VSR materials. This contributed to the formation of a double percolation structure induced by the addition of VSR to form an immiscible blend system with NRL matrix [22]. As the NRL/VSR blend ratio increased, the VSR acted as a spacer to induce the GNP-SDS nanofiller particles to pack denser at the interface and within the NRL matrix. This facilitated the formation of a conductive network and allowed more electrons to travel along the matrix to conduct electricity [23]. Thus, the electrical conductivity improved with the increment of the NRL/VSR blend ratio.

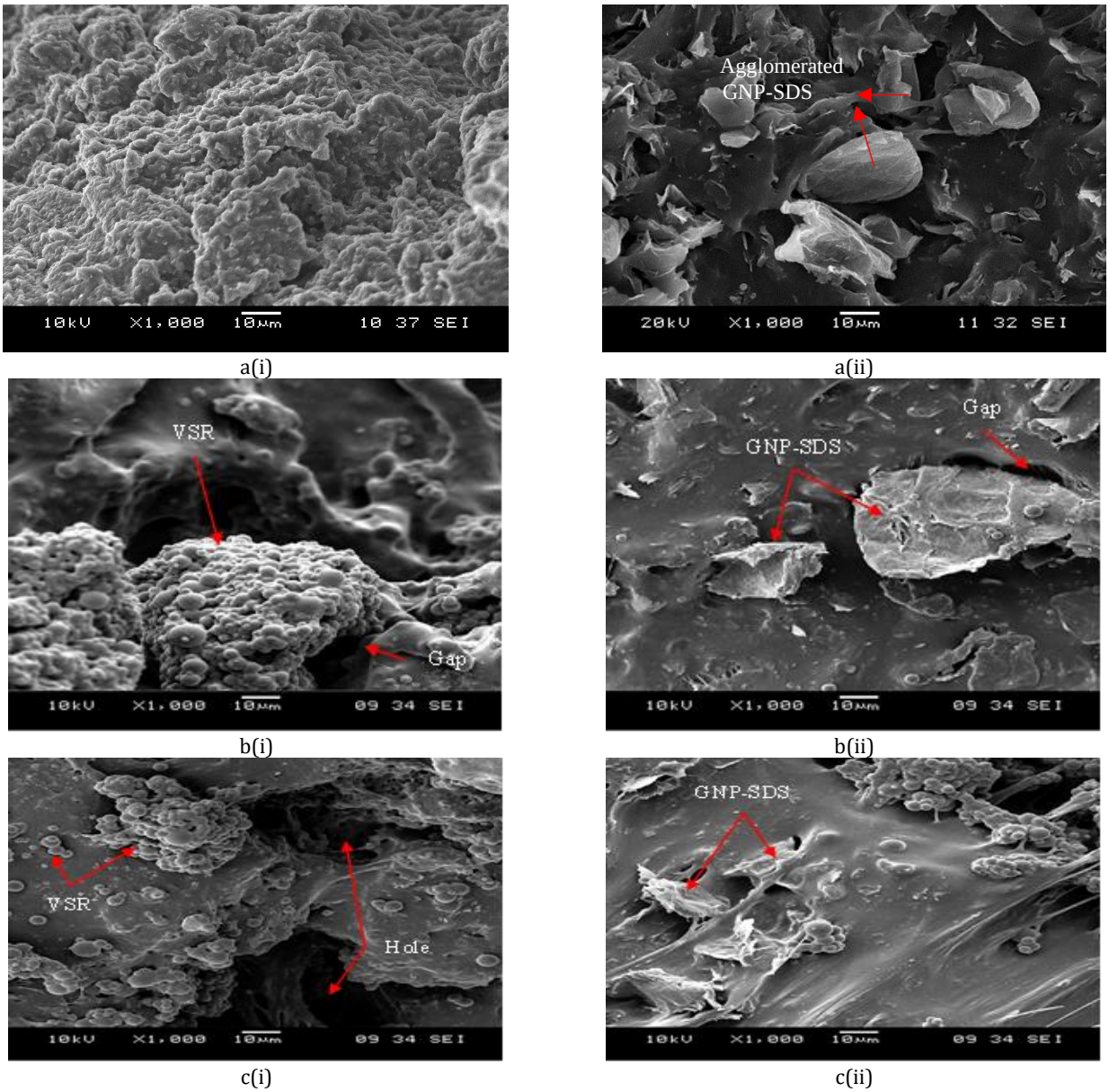

Figure 6 Tensile fractured surface of NRL/UVSR/GNP-SDS at blend ratios of (a) 100/0; (b) 95/5; and (c) 80/20 with (i) 0 phr and (ii) 7 phr of GNP-SDS, respectively, at ×1000 magnification.

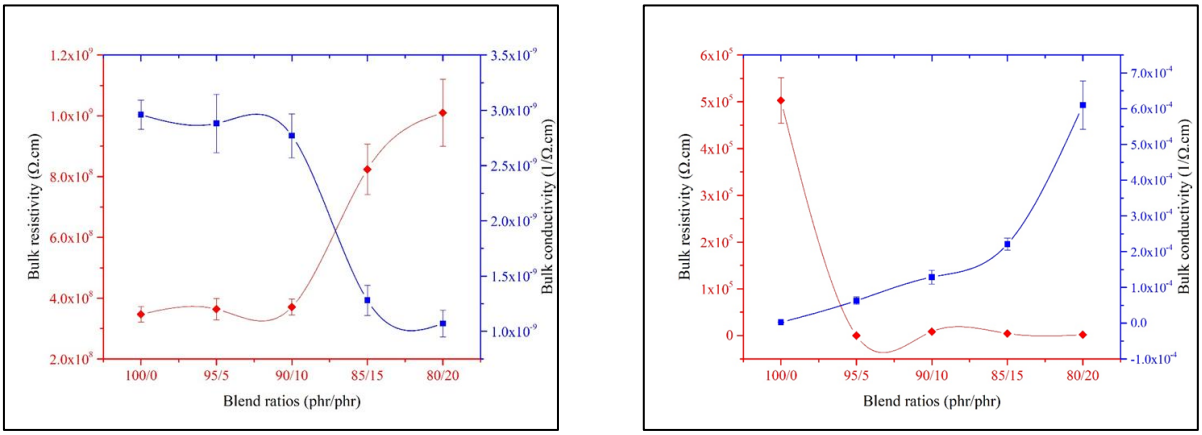

Figure 7 Electrical properties of (a) unfilled and (b) filled NRL/VSR with varying blend ratios.

5. CONCLUSION

This study was aimed at investigating the effect of blend ratios on the physical, mechanical, and electrical properties of the unfilled and filled NRL/VSR materials. It was found that these properties were affected by the interfacial strength of the blend components. In terms of physical properties, the solvent tended to swell the NRL phase due to the similar solubility parameter. Besides, the weak interfacial interaction between the blend components led to the solvent penetration as well as the stress concentration issues, resulting in the decrement of both physical and mechanical properties. In the case of the filled system, 7 phr of GNP-SDS tended to agglomerate due to the high van der Waals force between the adjacent GNP-SDS. Hence the specific surface area of the filler sheets reduced the stress transfer from the matrix to the filler phase for load bearing Consequently, the properties of the filled system displayed lower than the unfilled system. Interestingly, a double percolation structure formed between the immiscible NRL/VSR blend components, contributing to an enhancement in electrical conductivity as the blend ratio increased in the filled NRL/VSR materials. In summary, an increase in VSR content led to a reduction in mechanical properties due to weakened interfacial interactions but had a positive effect on electrical properties through the formation of a double percolation structure.

ACKNOWLEDGMENTS

The author would like to acknowledge the support from the Fundamental Research Grant Scheme (FRGS) under a grant number of FRGS/1/2018/TK05/UNIMAP/02/13 from the Ministry of Higher Education Malaysia.

REFERENCES

[1] S. Salaeh and P. Kao-ian, "Conductive epoxidized natural rubber nanocomposite with mechanical and electrical performance boosted by hybrid network structures," *Polymer Testing*, vol. 108, 2022.

[2] C. K. Yeoh, C. S. Cheah, R. Pushpanathan, C. C. Song, M. A. Tan, and P. L. Teh, "Effect of infill pattern on mechanical properties of 3D printed PLA and cPLA," in *IOP Conference Series: Materials Science and Engineering*, vol. 957, no. 124, 012064, 2020.

[3] K. Suppiah, P. L. Teh, S. Husseinsyah, R. Rahman, C. K. Yeoh, and C. W. Heng, "Materials Today: Proceedings," vol. 16, pp. 1611–1616, 2019.

[4] N. A. H. Jailudin and K. N. Mohd Amin, "Effect of curing temperature on cellulose nanocrystal reinforced natural rubber latex," *Journal of Chemical Engineering and Industrial Biotechnology*, vol. 6, no. 1, pp. 20–25, 2020.

[5] J. Xing, B. Deng, and Q. Liu, "Effect of graphene nanoplatelets on the performance of polyphenylene sulfide composites produced by melt intercalation," *High Performance Polymer*, vol. 30, no. 5, pp. 519–526, 2018.

[6] K. W. Kam, P. L. Teh, H. Osman, and C. K. Yeoh, "Characterization of different forms of vulcanized natural rubbers as elastomer spacer and toughening agent in two-matrix filled epoxy/natural rubber/graphene nano-platelets system," *Journal of Applied Polymer Science*, vol. 136, no. 11, 47198, 2019.

[7] K. W. Kam, P. L. Teh, H. Osman, and C. K. Yeoh, "Comparison study: effect of un-vulcanized and vulcanized NR content on the properties of two-matrix filled epoxy/natural rubber/graphene nano-platelets system," *Journal of Polymer Research*, vol. 25, no. 1, 2018.

[8] J. Morita, T. Goto, S. Kanehashi, and T. Shimomura, "Electrical double percolation of polybutadiene/polyethylene glycol blends loaded with conducting polymer nanofibers," *Polymers (Basel)*, vol. 12, no. 11, pp. 1–11, 2020.

[9] J. Ji et al., "Synthesis and characterization of room temperature vulcanized silicone rubber using methoxyl-capped MQ silicone resin as self-reinforced cross-linker," *Polymers (Basel)*, vol. 11, no. 7, 2019.

[10] J. L. Valentí, J. Carretero, M. Arroyo, and M. A. Lo, "Morphology/behavior relationship of

nanocomposites based on natural rubber/epoxidized natural rubber blends," *Composite Science Technology*, vol. 67, pp. 1330–1339, 2007.

[11] I. N. Indrajati and I. R. Dewi, "Performance of maleated castor oil-based plasticizer on rubber: Rheology and curing characteristic studies," in *IOP Conference Series: Material Science and Engineering*, vol. 223, no. 1, 2017.

[12] J. N. Lee, C. Park, and G. M. Whitesides, "Solvent compatibility of poly(dimethylsiloxane)-based microfluidic devices," *Analytical Chemistry*, vol. 75, no. 23, pp. 6544–6554, 2003.

[13] I. Khan, M. Mansha, and J. M. M. Abu, *Polymer blends*, Springer Nature Switzerland, 2019.

[14] W. Arayapranee and G. L. Rempel, "Properties of NR/EPDM blends with or without methyl methacrylate-butadiene-styrene (MBS) as a compatibilizer," *International Journal of Material & Structural Reliability*, vol. 5, no. 1, pp. 1–12, 2007.

[15] W. M. Che, P. L. Teh, J. A. Jalil, Y. C. Keat, and J. H. Lim, "The effect of liquid silicone rubber content on the properties of filled and unfilled natural rubber latex/liquid silicone rubber blend (NRL/LSR)," in *AIP Conference Proceedings*, vol. 2496, 2022.

[16] S. Ghorai et al., "Devulcanization of waste rubber and generation of active sites for silica reinforcement," *ACS Omega*, vol. 4, no. 18, pp. 17623–17633, 2019.

[17] P. Y. Foong et al., "Formation of polypropylene nanocomposite joint using silicon carbide nanowhiskers as novel susceptor for microwave welding," *Journal of Reinforced Plastics and Composites*, vol. 42, no. 9-10, pp. 413–429, 2023.

[18] R. M. Rosas, M. M. Genesca, J. O. Prat, A. Rahhali, and X. C. Fajula, "Dielectric, mechanical, and thermal characterization of high-density polyethylene composites with ground tire rubber," *Journal of Thermoplastic Composite Materials*, vol. 25, no. 5, pp. 537–559, 2011.

[19] "Properties and characterization of carboxymethyl cellulose/halloysite nanotube bio-nanocomposite films: Effect of sodium dodecyl sulfate," *Polymer Bulletin*, vol. 76, no. 1, pp. 365–386, 2019.

[20] G. C. Kabakçı, O. Aslan, and E. Bayraktar, "A review on analysis of reinforced recycled rubber composites," *Journal of Composite Science*, vol. 6, no. 8, 2022.

[21] N. Kamarudin, J. A. Razak, N. Mohamad, N. Norddin, and A. Aman, "Mechanical and electrical properties of silicone rubber based composite for high voltage insulator application," *International Journal of Engineering and Technology*, vol. 7, no. 3, pp. 452–457, 2018.

[22] J. L. Phua, P. L. Teh, S. A. Ghani, and C. K. Yeoh, "Influence of thermoplastic spacer on the mechanical, electrical, and thermal properties of carbon black filled epoxy adhesives," *Polymers of Advance Technologies*, vol. 28, no. 3, pp. 345–352, 2017.

[23] M. Zanoaga, Y. Mamunya, and F. Tanasa, "Conductive properties of some ternary thermoplastic nanocomposites filled with dispersed powders: A comparative study," *Revue R*, 2014.

.